

¹. Mohammed Y. FATTAH, ². Omar. F. S. al-DAMLUJI, ³. Yousif. J. al-SHAKARCHI

A PROCEDURE FOR DETERMINATION OF THE ALTERNAT MODEL PARAMETERS

¹. BUILDING AND CONSTRUCTION DEPARTMENT, UNIVERSITY OF TECHNOLOGY, IRAQ

²⁻³. CIVIL ENGINEERING DEPT., COLLEGE OF ENGINEERING, UNIVERSITY OF BAGHDAD, IRAQ

ABSTRACT: The ALTERNAT model described in this paper is a double hardening model for the mechanical behaviour of sand under alternating loading. For determination of the parameters of the ALTERNAT model, special types of triaxial tests are required, e.g., drained triaxial tests with monotonically increasing or decreasing axial strain and constant isotropic stress. These tests are not easy to be conducted in soil mechanics laboratories. It is intended here to choose a simple theoretical model to get the required stress - strain relationships for the determination of ALTERNAT model parameters. Of many theoretical models available to predict the overall response of sands, the endochronic model is chosen for this task. This model treats the sand as non-linear elastic-plastic material. Furthermore, the theory assumes inelastic changes to be caused only by the rearrangement of grains. The stress path required in the tests is applied in the computer program (ENDOCH) written by the authors. The parameters are calculated for two samples for which Ng and Dobry (1994) made experimental investigation. It is concluded that the proposed procedure for the determination of the ALTERNAT model parameters is successful. The stress-strain relations predicted are similar to those obtained by Molenkamp based on laboratory test results.

KEYWORDS: ALTERNAT model, endochronic, parameters, cyclic, sand

INTRODUCTION - The ALTERNAT Model

The model described in this paper forms the major component of a double hardening model for the mechanical behaviour of sand under alternating loading.

The model was developed by Molenkamp (1987) at Delft Geotechnics. In Figure (1), the yield surfaces of both plastic models, namely the "compressive" model and the "deviatoric" model are shown in the stress space of the isotropic stress, s , and the deviatoric stress, t .

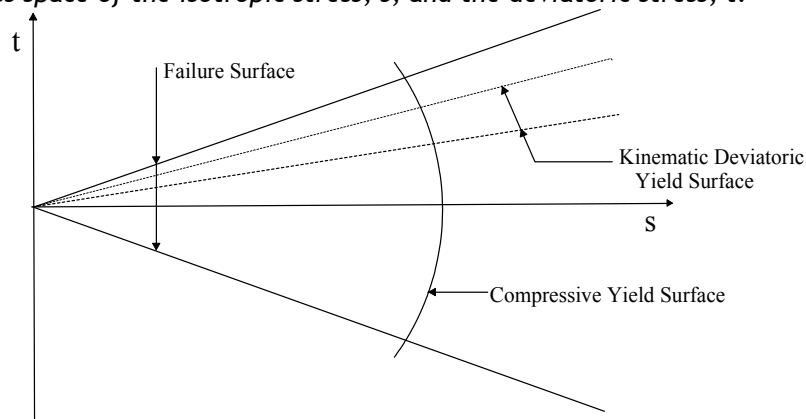


Figure 1 - The yield surfaces of the ALTERNAT model

Kinematic Plastic Model and Kinematic Rule

Using the elastic and plastic strains and the stress Σ together with their rates, the constitutive models in the current state can be defined on the Cartesian co-rotational base vectors, γ_i .

The elastic model will be of the form:

$$\Lambda_{ij} = \text{function} (\Sigma_{ij}) \quad (1)$$

The irreversible Eulerian strain rates or increments, \dot{K}_{ij} , are described by a plastic kinematic hardening model of the form:

$$K_{ij} = \frac{\frac{\partial G}{\partial \Sigma_{ij}} \frac{\partial F}{\partial \Sigma_{kl}} \Sigma^o_{kl}}{H} \tag{2}$$

$$T_{ij} = \Sigma_{ij} - \xi_{ij} : \text{pseudo stress} \tag{3}$$

in which: $F(T_{ij}, \chi) = 0$: yield surface, $G(T_{ij}, \chi_1) = 0$: plastic potential, $H(T_{ij}, \xi_{kl}, w_{mn}, \chi)$: hardening, w : plastic deformation, ξ_{ij} : tensor of anisotropy representing the effect of the anisotropic fabric, χ^0 : quantity describing the size of the kinematic yield surface; the so-called hardening parameter, and χ_1 : idem for plastic potential.

Figure (2) illustrates the above conditions.

Stress Induced Anisotropy Described By the Kinematic Hardening

For simplicity, the functional form of the kinematic hardening H_{kin} is chosen as follows:

$$H_{Kin} = H_{Kin}(I_T, \chi) \tag{4}$$

in which: I_T = invariants of the pseudo stress T_{ij} .

The kinematic hardening H_{kin} can be calculated from experimental data using the Equation:

$$H_{Kin} = \frac{\frac{\partial F^d}{\partial \sigma_{kl}} \sigma^o_{kl}}{K \cdot \dot{\gamma}^d} = \frac{\frac{\partial F^d}{\partial \sigma_{kl}} \sigma^o_{kl}}{\dot{\gamma}_{Kin}} \tag{5}$$

The curve of the shear stress level $(t/s)_c$ in drained triaxial compression at an isotropic pressure $(s/Pa) = 1$ (Pa is the atmospheric pressure) is related to the deviatoric strain (see Figure 3) by, (Molenkamp, 1985):

$$\left(\frac{t}{S}\right)_c = \frac{Y_1 Y_2}{(Y_1^n + Y_2^n)^{\frac{1}{n}}} \tag{6}$$

in which: t = shear stress, n = quantity larger than 1, and Y_1, Y_2 = two approximations of the shear stress level versus plastic deviatoric strain curve of drained triaxial compression at $s = Pa$.

Equation (6) has the properties that:

$$\left(\frac{t}{S}\right)_c \uparrow Y_1 \text{ if } Y_2 \gg Y_1$$

$$\left(\frac{t}{S}\right)_c \uparrow Y_2 \text{ if } Y_1 \gg Y_2$$

The two curves Y_1 and Y_2 are defined as follows:

$$Y_1 = E\chi^{EP} \tag{7}$$

and

$$Y_2 = \left(\frac{t}{S}\right)_{cv} + T \cdot \exp\{-\beta(\chi - \chi_t)\} \tag{8}$$

in which: E, EP = two parameters of the pre-peak fit by a power law. $(t/s)_{cv}$ = shear stress ratio in triaxial compression at the residual state, thus at very large strain χ .

$$T = Y_{2(\chi=\chi_t)} - \left(\frac{t}{S}\right)_{cv}$$

β = decay parameter.

The parameters E and EP of Equation (7) can be determined from the measured hardening curve when it is expressed in terms of $\ln(t/s)_c$ versus $\ln(\chi^p)$. A fit with a straight line to the low strain range of this plot reads:

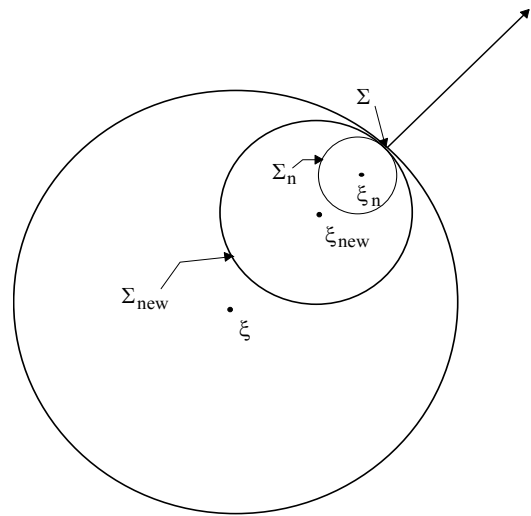


Figure 2 - Definition of the kinematic hardening and the motion of the kinematic yield surfaces

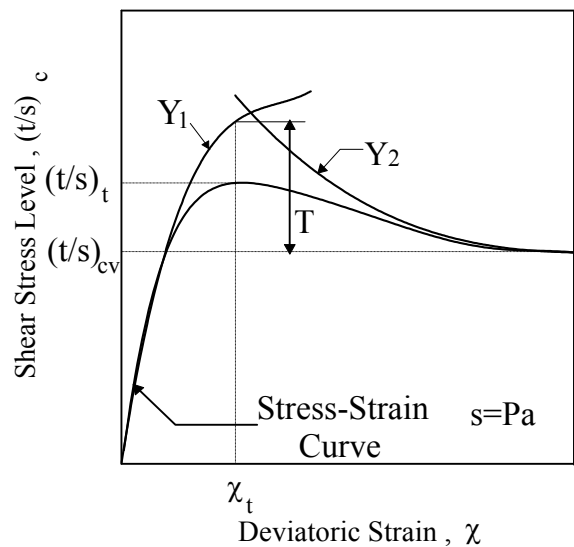


Figure 3 - Approximation for the stress-strain curve in drained triaxial compression test, (after Molenkamp, 1985).

$$\ln Y_1 = \ln E + EP \cdot \ln \chi \quad (9)$$

Next the parameters T and β can be determined from a plot of $\ln \left(\frac{t}{s} \right)_c - \left(\frac{t}{s} \right)_{cv}$ versus χ . A fit with a straight line to the large strain range reads:

$$\ln \left(\left(\frac{t}{s} \right)_c - \left(\frac{t}{s} \right)_{cv} \right) = \ln T - \beta (\chi - \chi_i) \quad (10)$$

For full description of the ALTERNAT model, refer to Molenkamp (1987) and Fattah (1999).

The Endochronic Model - Rearrangement Measure

The endochronic theory is a viscoplastic one but without introducing a yield surface. Therefore, all complexities and difficulties that develop in introducing a suitable yield criterion are avoided.

The source of inelasticity in sand is the irreversible rearrangement of grain configurations associated with deviatoric strains. Thus, it is convenient to characterize the accumulation of rearrangement by an appropriate variable, ξ , termed the rearrangement measure, which will be used as the independent variable in the stress - strain law.

Assuming that the development of inelastic strains is gradual, $d\xi$ must be a continuous and smooth function of $d\varepsilon_{ij}$. It can be shown that the only expression satisfying the above conditions is (Bazant and Krizek, 1976):

$$d\xi = \sqrt{J_2(d\varepsilon)} = \sqrt{\frac{1}{2} de_{ij} de_{ij}} \quad (11)$$

in which, $J_2(\)$ is the second invariant of the deviator of the tensor in parentheses, $\underline{\varepsilon} = [\varepsilon_{ij}]$ = the strain tensor.

$$e_{ij} = \varepsilon_{ij} - \delta_{ij} \frac{\varepsilon_{kk}}{3} \quad (12)$$

in which e_{ij} = the deviator of the tensor, δ_{ij} = Kronecker's delta.

Densification Due to Deviatoric Strains

The densification of sand may be characterized by the volumetric strain, λ , whose sign is chosen to be negative when the volume decreases. If vertical accelerations are not large enough to cause any significant separation or jumping of particles (as in the case in many earthquakes), the densification is produced almost exclusively by interparticle slips that result in a rearrangement of grain configurations.

Subject to this restriction, $d\lambda$ must be proportional to $d\xi$ and the dependence of the densification increment per cycle of shear on the strain amplitude and the number of cycles may be expressed by (Bazant and Krizek, 1976):

$$d_\lambda = - \frac{d_\kappa}{c(\kappa)} \quad (13)$$

$$d_\kappa = C(\varepsilon, \sigma) d\xi \quad (14)$$

in which: κ = the densification measure.

The function $c(\kappa)$ is the densification-hardening function that models the decrease in the densification increments per cycle with an increase in the number of cycles, N .

Expressing $c(\kappa)$ in a Taylor series and truncating it after the linear term yields:

$$c(\kappa) = c_0 (1 + \alpha \kappa) \quad (15)$$

in which α and c_0 are constants for a given sand at a given relative density.

The densification-softening function, $C(\underline{\varepsilon}, \underline{\sigma})$, may be regarded as a function of $J_2(\underline{\varepsilon})$ in addition to $I_1(\underline{\varepsilon})$ and $I_3(\underline{\varepsilon})$ which are the first and third invariants of $\underline{\varepsilon}$.

Accordingly, one suitable choice for $C(\underline{\varepsilon})$ is a function of $J_2(\underline{\varepsilon})$, and this function was identified by Bazant and Krizek (1976) as follows:

$$c(\varepsilon) = \frac{1}{2} q [4 J_2(\varepsilon)]^{(q-1)/2} \quad (16)$$

in which q is a non-negative constant for a given sand.

Generally, the material parameters α and q depend on the relative density, D_r . Based on the data reported by Silver and Seed (1971) and other data, Cuellar et al. (1977) proposed the following relationships:

$$C_0 = 1.0$$

$$q = -0.95 D_r^2 + 2.33 D_r + 0.54 \quad (17)$$

$$\alpha = -33.33 D_r^2 + 61.66 D_r - 20 \quad (18)$$

in which, D_r is expressed as a number (not a percentage).

Intrinsic Time

Since the increments of irreversible (inelastic) strains are caused by interparticle slips, they must be proportional to increments of the rearrangement measure, ξ , and the proportionality coefficient may, in general, depend on the state of strain and stress.

To express this fact, a new independent variable, η , may be expressed such that:

$$d\eta = F(\varepsilon, \sigma) \cdot d\xi \quad (19)$$

As in the case of densification, the increment of inelastic strain per cycle diminishes as the number of cycles increases. To account for this effect, it is expedient to introduce a new independent variable, ζ , termed intrinsic time, whose growth relative to η or ξ gradually diminishes. This phenomenon may be described by the relation:

$$d\zeta = \frac{d\eta}{f(\eta)} \quad (20)$$

in which $f(\eta)$, which may be termed a strain-hardening function, is a continuously increasing positive function of η and is given by the relation:

$$d(\eta) = \left(1 + \frac{\beta}{r} \eta\right)^r \quad (21)$$

in which β and r are constants.

The function F is a strain-softening function and $f(\eta)$ is a strain-hardening function in the sense of causing a decrease or increase in the slope of the stress - strain curve.

However, within the range of strains commonly encountered in seismic loading, it appears that F may be equal to unity as an acceptable approximation, (Bazant and Krizek, 1976).

Endochronic Stress-Strain Law for Sand

Because of the limited range of ξ -values that are of practical interest, it had been shown by Bazant and Krizek (1976) that the deviatoric stress - strain relation may be approximated by:

$$de_{ij} = \frac{dS_{ij}}{2G} + de_{ij}^p \quad (22a)$$

$$de_{ij}^p = \frac{S_{ij}}{2G} + \frac{d\xi}{Z_1} \quad (22b)$$

in which: G = shear modulus, e_{ij} , e_{ij}^p = the elastic and inelastic deviatoric strains, Z_1 = constant (analogous to the relaxation time in a Maxwell chain used in viscoelasticity).

The volumetric stress - strain relation may be written as:

$$d\varepsilon = \frac{3\sigma}{3K} + d\lambda \quad (23)$$

in which: K = the bulk modulus.

For a wide range of shear strains and confining pressures, Cuellar et al. (1977) found, using simple shear tests, the following values for the parameters:

$$Z_1 = 2.5 \times 10^{-4}, \quad \beta = 2.0 \quad \text{and} \quad r = 0.70$$

Equations (22) and (23) are capable of describing experimental results quite well within a range of shear strain amplitude from about 0.0001 to 0.0005, but the agreement is not good for a boarder range of amplitudes, (Cuellar et al., 1977).

To get better agreement, G should be assumed to depend on $I_1(\underline{\sigma})$, the first invariant of $\underline{\sigma}$,

since that the elastic rigidity of the solid skeleton depends on the number and areas of interparticle contacts, which in turn depends on $I_1(\underline{\sigma})$.

Since the contact areas between grains increase with the confining stress, the solid skeleton becomes stiffer and grain contacts slip as the confining stress is increased. Based on extensive experimental data for the dynamic shear modulus, G had been shown to be essentially proportional to the square root of the confining stress. Accordingly, Bazant and Krizek (1976) proposed the following expression for the shear modulus, G :

$$G = \sqrt{M \sigma_v'} \quad (24)$$

in which: σ'_v = vertical effective stress, M = constant that is equal to 0.01 kN/m² based on the simple shear tests conducted by Cuellar et al. (1977).

It was found by Cuellar et al. (1977) that Equation (24) did not suffice to adequately describe the data for large strain amplitudes; generally the unloading portions of these hysteresis loops were too steep.

It is recommended here to use a new procedure based on the procedure adopted by Huang and Chen (1990) for the cap plasticity model in which the elastic bulk modulus, K , can be derived from the confined compression test as follows:

$$K = \frac{d\bar{P}}{d\varepsilon_v^e} = \frac{\bar{P}}{A_e} \tag{25}$$

with

$$A_e = \frac{G_r}{2.303(1+e_i)} \tag{26}$$

where: C_r = the swelling index, \bar{P} = effective hydrostatic stress, ε_v^e = elastic volumetric strain.

The elastic shear modulus, G , can be determined if Poisson's ratio, ν , is evaluated:

$$G = \frac{3K(1-2\nu)}{2(1+\nu)} \tag{27}$$

DETERMINATION OF THE ALTERNAT MODEL PARAMETERS

The double hardening kinematic model ALTERNAT consists of three different model components, namely:

- (1) Non-linear elastic model.
- (2) Plastic compressive model.
- (3) Plastic deviatoric kinematic model.

It was shown by Molenkamp (1980) that the parameters A , AP , B and BP of the elastic model can be determined most easily from a drained isotropic loading-unloading test. The parameter V can be determined from the behaviour during initial deviatoric unloading.

If it could be assumed that the material is isotropic initially, then from one drained triaxial test at constant isotropic stress $s = Pa$ and monotonically increasing axial deformation (see Figure 4a and b) the following parameters can be determined. This must be done after the elastic strains and the plastic compressive strains have been subtracted from the stress - strain curves.

E and EP parameters can be determined from the fit by a power law to the first part of the curve in Figure (4a). The parameters χ_{t_0} , $(t/s)_{cv}$, T and β are determined from the fit by an exponential function to the last part of the same curve (see Figure 4a).

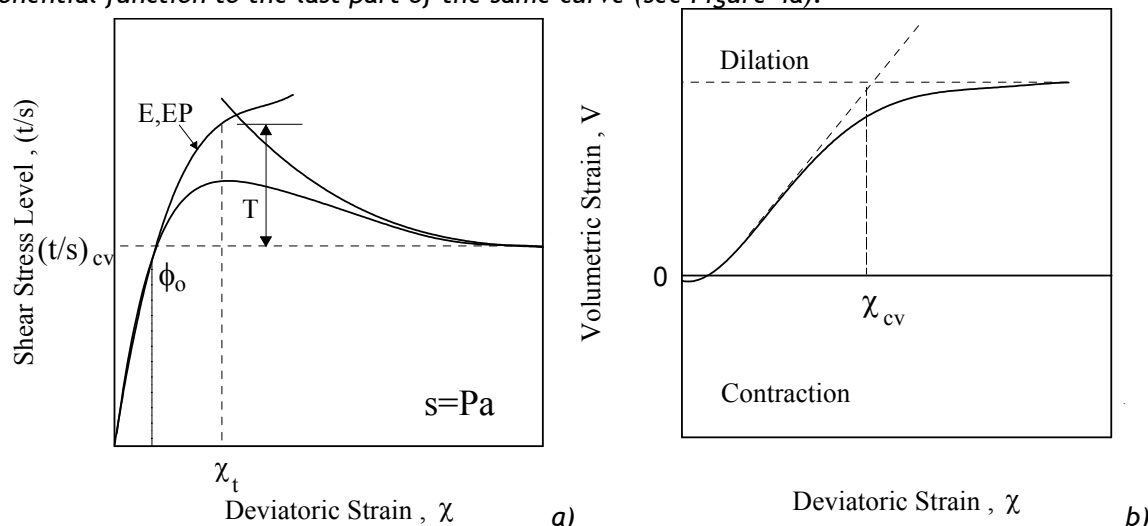


Figure 4 - Determination of the ALTERNAT model parameters from drained triaxial test at constant isotropic stress.

In the case of only one test and no other published experimental data on similar materials, only one dilatancy angle ϕ_0 can be derived from the curve of the isotropic strain versus deviatoric strain (see Figure 4b). Then it must be assumed that $FIMU(\phi_{it}) = FICV(\phi_{cv}) = \phi_0$. In such a case, the parameter $SCV(S_{cv})$ is not relevant and can be put at $S_{cv} = 1$.

From this curve (Figure 4b) also the parameter $CHICV(\chi_{cv})$ can be determined if the deformation remains uniform until large deformation.

For a proper determination of the parameters ϕ_{μ} , ϕ_{cv} , S_{cv} , LB and COH (c), at least two drained triaxial compression tests at different constant isotropic stresses would be needed. From each individual test, a dilatancy angle ϕ_0 can be calculated. Next the parameters ϕ_{μ} , ϕ_{cv} and S_{cv} can be fitted using the values of ϕ_0 .

The determination of the parameters E, EP, EE and EEP is most simple in case of initial isotropy of the sample. The parameters E and EP are determined from the data of a triaxial compression test at constant isotropic stress following directly Equation (7).

The parameters EE and EEP can be determined from a drained triaxial extension test at constant isotropic effective stress as shown in Figure (5). To this end, to the measured shear stress level $(t/s)_e$ in triaxial extension there exists an equivalent shear stress level $(t/s)_c$ in triaxial compression with the same measure of shear stress level f^d for triaxial compression and:

$$F^d = 27 \left\{ \frac{1}{(1 - \sqrt{2} \left(\frac{t}{s}\right)_e) \left(1 + \frac{1}{\sqrt{2}} \left(\frac{t}{s}\right)_e\right)^2} - 1 \right\} - f^d \quad (28)$$

for triaxial extension.

Then the initial part of the resulting stress - strain curve can be fitted as (see Figure 5):

$$\chi_e = EE \left(\frac{t}{s} \right)_c^{EEP} \quad (29)$$

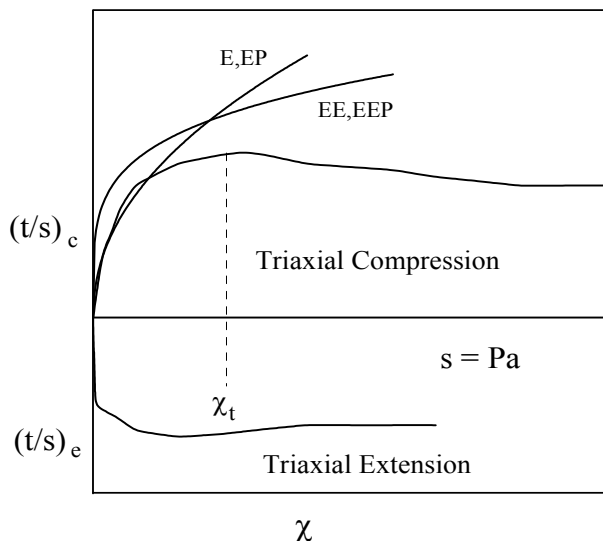


Figure 5 - Determination of the parameters E, EP, EE and EEP from triaxial compression and extension tests

For the determination of tensile strength PTENS in isotropic loading, either a hydraulic fracturing test or tensile test must be performed.

For the determination of viscosity VC at liquefaction, strain controlled liquefaction tests at different rates must be performed.

Summary of Required Tests

For easy determination of all parameters of an initially isotropic material, the following tests would be needed:

- 1 drained isotropic loading-unloading test.
- 1 (or more) drained triaxial compression test(s) with monotonically increasing axial strain at different constant isotropic stresses.
- 1 (or more) drained triaxial extension test(s) with monotonically decreasing axial strain at different constant isotropic stresses.
- 1 (or more) drained triaxial test(s) with different cyclic deviatoric stress t and constant isotropic stress s .
- 1 hydraulic fracture test.
- 1 (or more) strain controlled undrained triaxial compression test(s) leading to liquefaction.
- In situ K_0 test or strain controlled triaxial compression with zero lateral strain on undisturbed sample.

Stress Path

Molenkamp (1987) described a procedure for the determination of most of the model parameters from a drained triaxial test on apparently initially isotropic Eastern Scheldt sand with $d_{50} = 150 \mu\text{m}$ and initial porosity $n = 0.40$. The stress path of the test involved:

- isotropic loading up to a 2 bar cell pressure.
- isotropic unloading back to 1 bar cell pressure.
- 3 cycles of deviatoric loading at a constant isotropic pressure of 1 bar.
- isotropic loading up to 4 bar and unloading to 1 bar.
- another cycle of deviatoric loading at a constant isotropic pressure of 1 bar.
- loading towards failure at constant isotropic stress.

THE PROPOSED PROCEDURE FOR THE DETERMINATION OF ALTERNAT MODEL PARAMETERS

The stress path described in the previous section will be applied in the computer program (ENDOCH) written by the authors with some equations of the ALTERNAT model. The procedure will be illustrated through the following example.

Ng and Dobry (1994) made experimental and theoretical investigation on granular specimens composed of uniform spheres.

The discrete element method (DEM) was used in simulating round uniform quartz sand under monotonic drained loading with constant mean stress and cyclic constant volume loading (undrained).

A typical 2-dimensional specimen used by Ng and Dobry (1994) is shown in Figure (6). The porosity was calculated as the ratio between the pore area of the plane where the spheres' centers lie and the box dimensions. In general 3-dimensional specimens, the porosity was defined as $n = 1 - \frac{\sum \text{volume of spheres}}{\text{volume of box}}$.

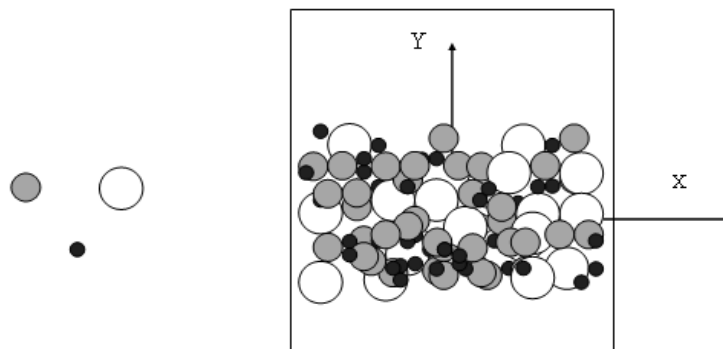


Figure 6 - Geometry of 2-dimensional specimen used by Ng and Dobry (1994)

Two simulated granular specimens composed of spheres were used in this study (specimens B and C). All particles were assigned the properties of quartz: shear modulus, $G = 28.957 \text{ MPa}$, Poisson's ratio, $\nu = 0.15$, and the friction coefficient $\mu_s = \tan \phi_0 = 0.5$ where ϕ_0 is the interparticle friction angle.

The specimens are described in Table (1) in which the third and fourth columns show the total number of spherical particles N used in each specimen, as well as the ratios $R_1/R_2/R_3$ of three different particle sizes with $N_1/N_2/N_3$ which are the numbers of particles having these sizes.

Table 1 - Characteristics of specimens used in simulation, (from Ng and Dobry, 1994).

Specimen	μ_s	Number and Sizes of Spheres in Specimens		Specimen after Consolidation		
		Total Number of Particles	$(N_1/N_2/N_3)$ and $(R_1/R_2/R_3)$	σ_c (kPa)	Porosity (n)	Relative Density (%)
B	0.5	398	291/79/28 (1/1.5/2)	137	0.349	68.8
C	0.5	398	291/79/28 (1/1.5/2)	137	0.382	52.0

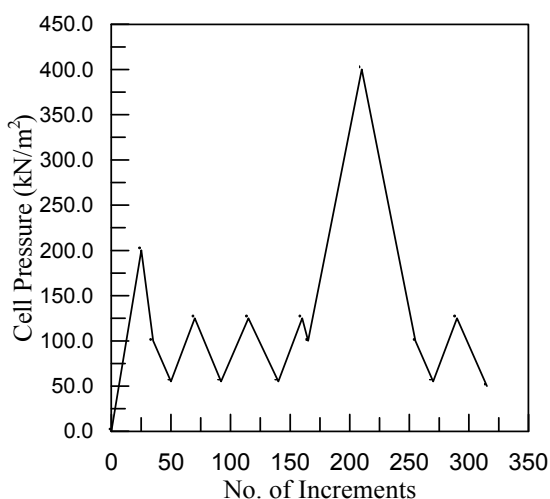


Figure 7 - The cell pressure against number of increments for the stress path followed by numerical simulation

In Figure (8), the effective stress path is shown in terms of:

$$s = (\sigma_a + 2\sigma_r) \sqrt{\frac{1}{3}} \quad (30)$$

$$t = (\sigma_a - \sigma_r) \sqrt{\frac{2}{3}} \quad (31)$$

where: σ_a = axial stress, σ_r = radial stress.

Zero-Dilatancy Rule

Dilatancy is independent of the increment of stress or its direction for a fixed stress point, and can be approximated by a linear function of stress ratio, (Zienkiewicz et al., 1987):

In all cases, $N = N_1 + N_2 + N_3$ and all the specimens were isotropically consolidated to $\sigma_c = 137 \text{ kPa}$ prior to monotonic and cyclic loading.

In the following steps, the ALTERNAT model parameters will be calculated for specimen B. In Figure (7), the cell pressure (σ_c) is shown against the number of data points (each point concerns with a loading increment). It should be noticed that the afore mentioned stress path consists of many increments of load, each followed by an unloading and reloading increment.

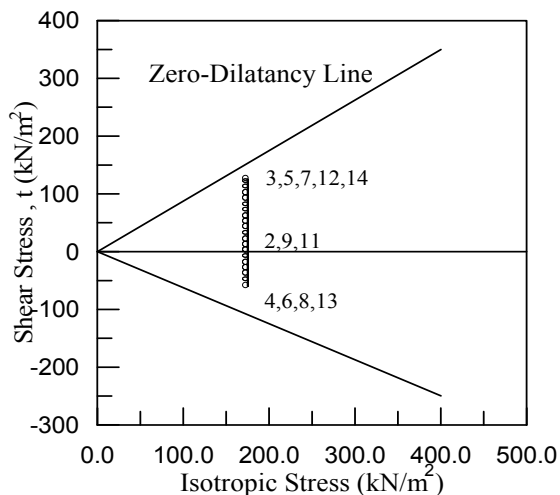


Figure 8 - The effective stress path followed by the numerical simulation

$$dg = \frac{\dot{V}}{\dot{\gamma}} = (1 + \alpha_g) (M_g - \eta) \tag{32}$$

where: $\eta = t/s$ and α_g is constant.

This simple rule predicts zero dilatancy whenever the line:

$$\eta = M_g \tag{33}$$

is reached.

Generalization to three-dimensional stress conditions can be done if a law of a Mohr-Coulomb type is assumed (Zienkiewicz and Pande, 1977) for the zero dilatancy line, giving (Zienkiewicz et al., 1987):

$$M_g = 6 \sin \phi_{cv} / (3 - \sin \phi_{cv} \sin 3\theta) \tag{34}$$

where θ is Lode's angle defined by Molenkamp (1987) as:

$$\sin 3\theta = 3\sqrt{6} \frac{J_{3\tau_{ij}}}{t^3}, \quad -\frac{\pi}{6} \leq \theta \leq \frac{\pi}{6} \tag{35}$$

where: ϕ_{cv} = a constant residual angle of friction, J_3 = the third invariant of the deviatoric pseudo stress tensor.

In Figure (8), the zero-dilatancy lines were drawn depending on the equation of Zienkiewicz et al. (1987), i.e., Equation (34). The numbers in this figure indicate the sequence of loading.

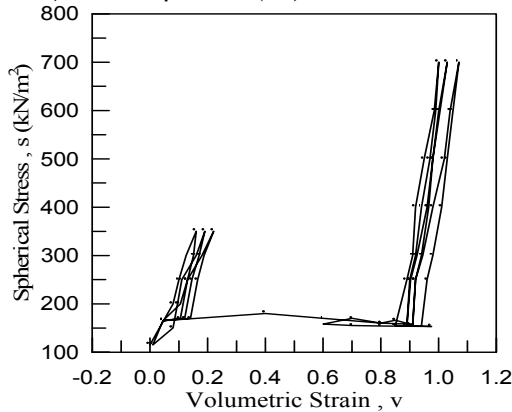


Figure 9 - Stress - strain path of the isotropic components of s and v

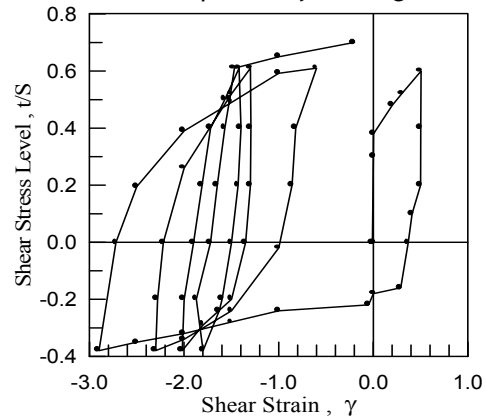


Figure 10 - The shear stress level against shear strain for the numerical simulation

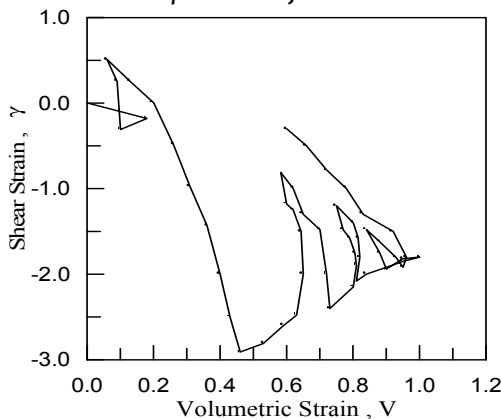


Figure 11 - The strain path in terms of shear strain and spherical strain

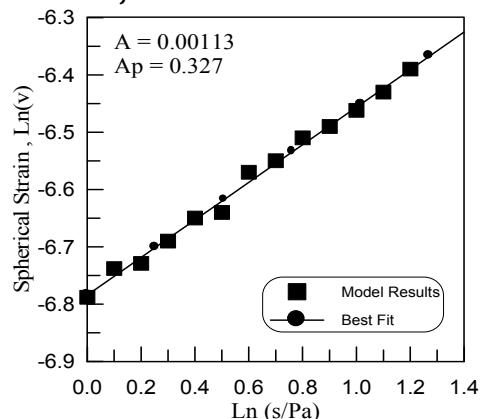


Figure 12 - Calculation of elastic parameters A and AP through logarithmic correlations

In Figure (9), the stress - strain path of the isotropic components are shown in terms of s and the spherical (volumetric) strain:

$$V = \frac{-1}{\sqrt{3}} \ln \left(\frac{V_o + \Delta V}{V_o} \right) \tag{36}$$

in which: V_o = the initial volume of the sample.

In Figure (10), the shear stress level (t/s) is shown against the shear strain γ :

$$\gamma = \left\{ -3 \ln \left(\frac{h_o + \Delta h}{h_o} \right) + \ln \left(\frac{v_o + \Delta v}{v_o} \right) \right\} \sqrt{\frac{1}{6}} \tag{37}$$

in which: h_o = initial height of the sample = 76 mm.

In Figure (11), the strain path is shown in terms of the shear strain γ and the spherical strain V . It should be noticed that mainly due to cyclic loading, a permanent volumetric strain and a shear strain are generated. The ratio of the rate of change of the volumetric strain and the shear strain, $\dot{V} / \dot{\gamma}$, in consecutive cycles is quite similar.

The parameters A and AP can be calculated from an isotropic loading test. In Figure (12), the relevant data are put in the form of the logarithms of V and (s/Pa) , which should be linear. This relation is approximated by:

$$V = A \left(\frac{s}{Pa} \right)^{AP} \tag{38}$$

The best fit of the relation gives: $A = 0.00113$ and $AP = 0.327$.

Knowing the parameters A and AP for a range of magnitudes of the parameter V , the stress - strain response was calculated. Next from the calculated strains as given in Figures (9) and (11), the elastic strains, which were calculated using the calculated parameters, were subtracted. The remaining plastic components are shown in Figures (13), (14) and (15).

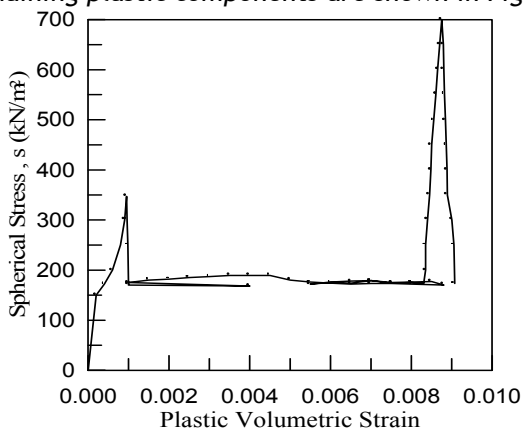


Figure 13 - Spherical stress against plastic component of strain

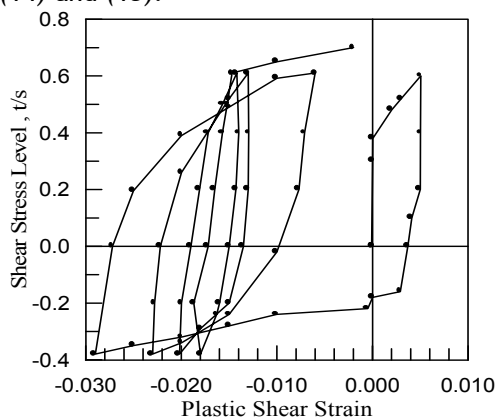


Figure 14 - Shear stress level against plastic shear strain for the numerical simulation

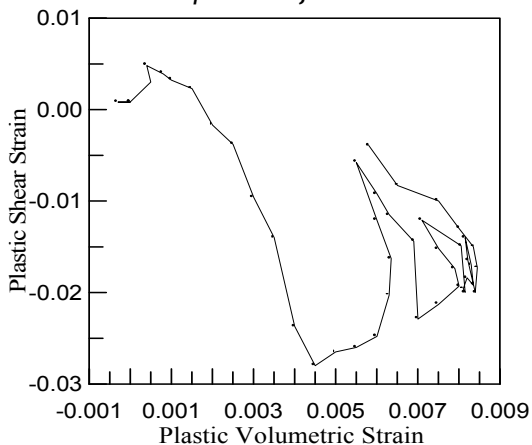


Figure 15 - Plastic spherical strain against plastic shear strain

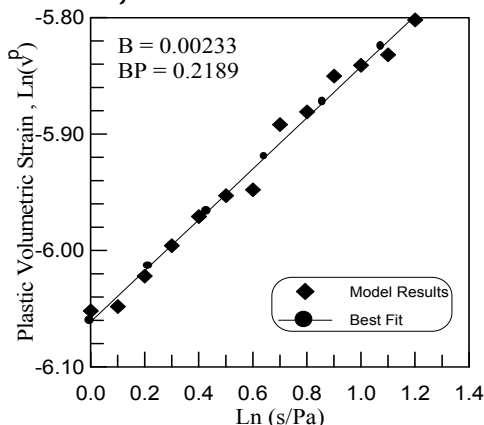


Figure 16 - Calculation of elastic parameters B and BP through logarithm correlations

Then using the remaining stress - plastic strain path of the initial loading of Figure (13), the parameters B and BP were calculated. To this end, the initial loading path in Figure (13) is approximated by the expression:

$$V = B \left(\frac{s}{Pa} \right)^{BP} \tag{39}$$

In Figure (16), the relevant data are put in the form of the logarithms of V and (s/Pa) which should be linear. The best fit of the relation gave the magnitudes of B and BP as follows: $B = 0.00233$ and $BP = 0.2189$.

The experimental data of the shear stress level (t/s) and the deviatoric plastic strain γ^d (Figure 14) can be used for the determination of:

- 1- the load history parameters κ and n_d .
- 2- the parameters of the hardening E , EP , EE and EEP .
- 3- the initial anisotropic condition in case the material is not isotropic initially.

Due to the straight envelopes of the alternating strain path of Figure (15), κ could be chosen equal to 1, (Molenkamp, 1987).

In Figure (17), the resulting kinematic shear strain γ_{kin}^d from the stress reversal are shown as a function of the shear stress level (t/s).

Cyclic Mobility

It can be seen in Figure (17) that the average resulting kinematic deviatoric strain γ_{kin}^d of loading is slightly larger than the similar strain of unloading. This difference can be contributed to the cyclic mobility.

$$\Delta\gamma_{mob} = \Delta\gamma_{loading} - \Delta\gamma_{unloading} \tag{40}$$

It can also be noticed that the shapes of the curves of loading and unloading are different. The curve for loading shows a continuously decreasing tangent stiffness immediately from the start, while for the unloading curve the tangent stiffness remains quite large during the first part of the unloading path and then starts to decrease much faster than the curve for loading. This is also illustrated in Figure (18).

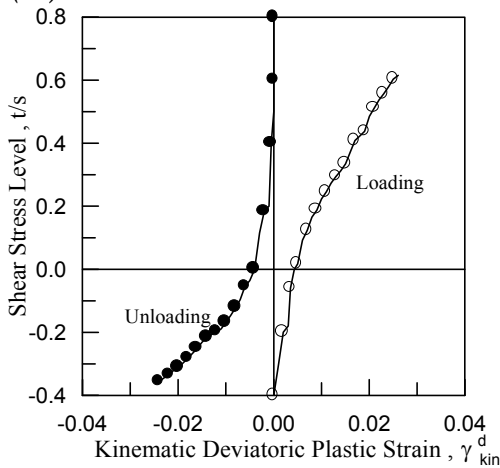


Figure 17 - Kinematic deviation plastic strain in cyclic loading from stress reversal against shear stress level

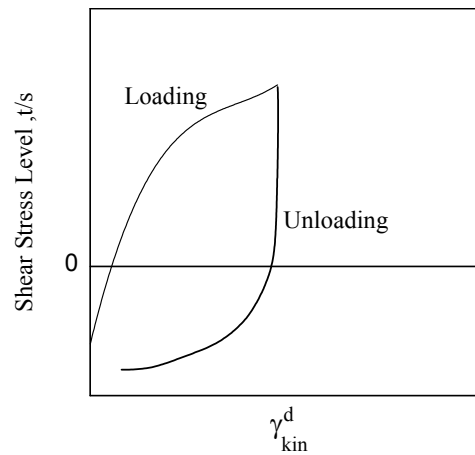


Figure 18 - Cyclic mobility

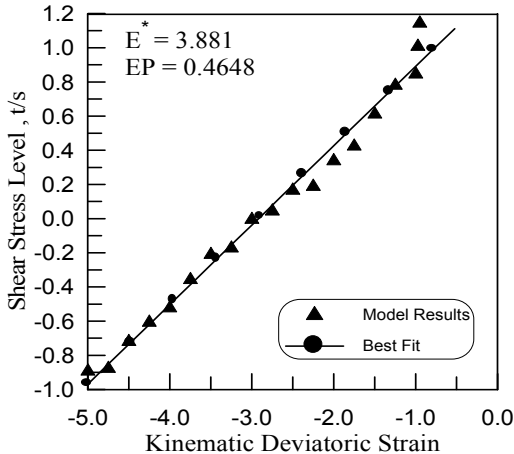


Figure 19 - Linear approximation to logarithm shear stress level against kinematic deviatoric strain, loading

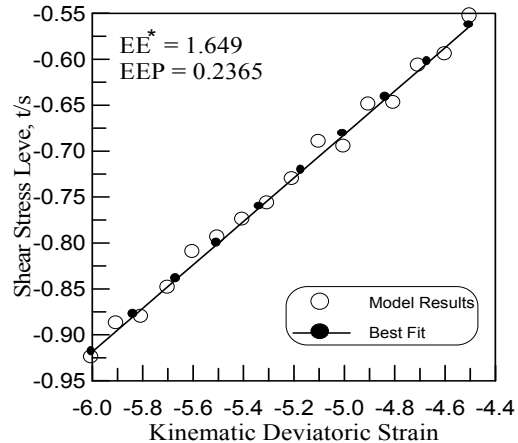


Figure 20 - Linear approximation to logarithm shear stress level against kinematic deviatoric strain, unloading

At this stage still the hardening parameters for triaxial compression E and EP and for triaxial extension E and EEP . The fit to the stress - strain curve for triaxial compression can be obtained by using for the shear stress level below peak the following expression:

$$\left(\frac{t}{s}\right)_c = E^* \left\{ \gamma_{kin,c}^d \right\}^{EP} \tag{41}$$

In Figure (19), the best linear fit for shear stress levels between zero and peak of the logarithms of $\gamma_{kin,c}^d$ and $(t/s)_c$ is shown. The fit gave the following values:

$$E^* = 3.881 \text{ and } EP = 0.4648$$

It is assumed that the deviatoric strain rate, $\dot{\gamma}_c^d$, in a drained triaxial compression test is related to the deviatoric strain rate $\dot{\chi}$ at the same stress level $(t/s)_c$ by, (Molenkamp, 1987):

$$\dot{\gamma}_{kin,c}^d \left(\frac{s}{Pa} \right)^{LB} \dot{\chi} \tag{42}$$

in which: LB = parameter of the order 0.1 up to 0.5.

From Equation (42) it follows, if LB = 0.3, that:

$$E = E^* \left(\frac{s}{Pa} \right)^{(LB*EP)} = 3.881(\sqrt{3})^{0.3*0.4648} = 4.19$$

The fit to the equivalent curve for triaxial extension is expressed by:

$$\left(\frac{t}{s} \right)_c = E E^* \left\{ \dot{\gamma}_{kin,e}^d \right\}^{EEP} \tag{43}$$

In Figure (20), the best linear fit for high shear stress levels to the logarithms of $\dot{\gamma}_{kin,e}^d$ and $(t/s)_c$ is shown. The fit gives the following values:

$$EE^* = 1.649 \text{ and } EEP = 0.2365.$$

From Equation (42), it follows, if LB = 0.3, that:

$$EE = EE^* \left(\frac{s}{Pa} \right)^{(LB*EP)} = 1.649(\sqrt{3})^{0.3*0.2365} = 1.71$$

In Figure (21), the average equivalent curves for triaxial compression and extension are shown together. Figure (22) shows the relationship between volumetric and shear strains from which the parameter $\chi_{cv} = 1$.

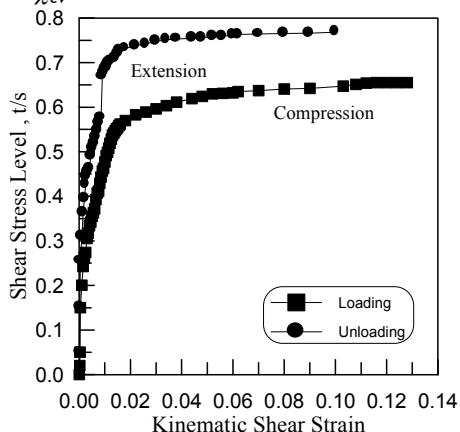


Figure 21 - Kinematic deviatoric strain in cyclic loading from stress reversal against shear stress level

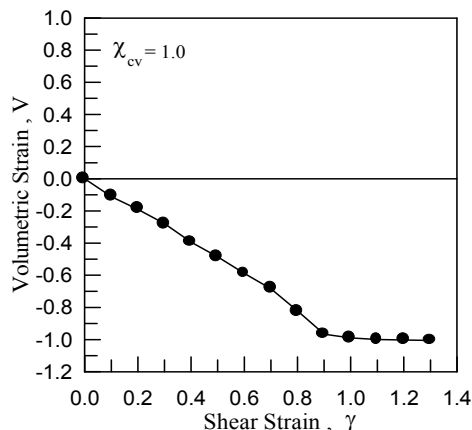


Figure 22 - Shear strain against volumetric strain

Table (2) - ALTERNAT model parameters for the specimens used by Ng and Dobry (1994) as determined by the proposed procedure.

Parameter		Value	
		Specimen B	Specimen C
Non-linear Elastic Model:	V	0.12	0.12
	A	0.00113	0.00112
	AP	0.327	0.348
Deviatoric Plastic Model: Hardening for Triaxial compression:	E	4.19	4.17
	EP	0.4648	0.4633
	CHIT (χ_t)	0.116	0.122
	TSINF (t/s) _{cv}	0.655	0.643
	TT (T)	0	0
	BET (β)	0	0
	CHIM (χ_m)	0.049 (Molenkamp, 1987)	0.049 (Molenkamp, 1987)
	NM (n_m)	5.15 (Molenkamp, 1987)	5.15 (Molenkamp, 1987)
	LB	0.3 (published data)	0.3 (published data)
Hardening for Triaxial Extension:	COH (c)	0	0
	EE	1.71	1.69
Hardening by Densification:	EEP	0.2365	0.2314
	POROS (n_i)	0.349	0.382
	DENSE (n_d)	0.27	0.27
Dilatancy:	KAP (κ)	1.	1.
	FIMU (ϕ_{i1})	26.5°	26.5°
	FICV (ϕ_{cv})	26.5°	26.5°
	SCV (S_{cv})	1.	1.
Tensile Strength: PTENS (σ_t)	CHICV (χ_{cv})	1.	1.
		0.	0.
Viscosity in Liquefaction: VC (V_c)		0.01 sec.	0.01 sec.
Initial State:	CHII (χ_l)	0.05	0.05
	K _o	0.55	0.55

The other parameters may be assumed on the basis of published experimental data of similar materials.

The same procedure was followed for the determination of the parameters for specimen C. The whole parameters are listed in Table (2).

CONCLUSIONS

For determination of the parameters of the ALTERNAT model, special types of triaxial tests are required, e.g., drained triaxial tests with monotonically increasing or decreasing axial strain and constant isotropic stress. These tests are not easy to be conducted in soil mechanics laboratories. It is intended here to choose a simple theoretical model to get the required stress - strain relationships for the determination of ALTERNAT model parameters.

Of many theoretical models available to predict the overall response of sands, the endochronic model is chosen for this task.

The stress path required in the tests is applied in the computer program (ENDOCH) written by the authors. The parameters are calculated for two samples for which Ng and Dobry (1994) made experimental investigation.

It is concluded that the proposed procedure for the determination of the ALTERNAT model parameters is successful. The stress-strain relations predicted are similar to those obtained by Molenkamp based on laboratory test results.

REFERENCES

- [1] Bazant, Z. P. and Krizek, R. J., (1976). (Endochronic Constitutive Law for Liquefaction of Sand), *Journal of Engineering Mechanics*, ASCE, Vol. 102, EM2, p. p. 225 - 238.
- [2] Cuellar, V., Bazant, Z. P., Krizek, R. J. and Silver, M. L., (1977). (Densification and Hysteresis of Sand Under Cyclic Shear), *Journal of Geotechnical Engineering Division*, ASCE, Vol. 103, ýGT5, p. p. 399 - 416.
- [3] Fattah, M. Y., (1999). (The Non-Linear Dynamic Behaviour of Soils), Ph.D dissertation, University of Baghdad.
- [4] Huang, T. K. and Chen, W. F., (1990). (Simple Procedure for Determining Cap-Plasticity Model Parameters), *Journal of Geotechnical Engineering Division*, ASCE, Vol. 116, No. 3, p. p. 492 - 513.
- [5] Molenkamp, F., (1980). (Elasto-Plastic Double Hardening Model, MONOT), Report, Delft Geotechnics.
- [6] Molenkamp, F., (1985). (A Stress-Strain Curve for Both Hardening and Softening), *Proceedings of the International Conference on "Numerical Methods in Engineering NUMETA85"*, Swansea, p.p. 489-496.
- [7] Molenkamp, F., (1987). (Kinematic Model for Alternating Loading, ALTERNAT), Report, Delft Geotechnics.
- [8] Ng, T. T. and Dobry, R. (1994). (Numerical Simulation of Monotonic and Cyclic Loading of Granular Soil), *Journal of Geotechnical Engineering Division*, ASCE, Vol. 120, GT2, p.p. 388-403.
- [9] Silver, M. L. and Seed, H. B., (1971). (Volume Changes in Sands During Cyclic Loadings), *Journal of Soil Mechanics and Foundations Division*, ASCE, Vol. 97, SM9, p. p. 1171 - 1182.
- [10] Zienkiewicz, O. C. and Pande, G. N., (1977). (Some Useful Forms of Isotropic Yield Surfaces for Soil and Rock Mechanics), Chapter 5 in "Finite Elements in Geomechanics", edited by G. Gudehus, p.p. 179-190.
- [11] Zienkiewicz, O. C., Chan, A. H., Pastor, M. and Shiomi, T., (1987). (Computational Approach to Soil Dynamics), in "Soil Dynamics and Liquefaction", edited by A. S. Cakmak, (Developments in Geotechnical Engineering-42), p.p. 3-13.



ANNALS of Faculty Engineering Hunedoara



- International Journal of Engineering

copyright © UNIVERSITY POLITEHNICA TIMISOARA,
FACULTY OF ENGINEERING HUNEDOARA,
5, REVOLUTIEI, 331128, HUNEDOARA, ROMANIA
<http://annals.fih.upt.ro>